Journal of Structural Biology **137,** 194–205 (2002)
doi:10.1006/jsbi.2002.4468

PEVK Domain of Titin: An Entropic Spring with Actin-Binding Properties

Wolfgang A. Linke,*[,1] Michael Kulke,* Hongbin Li,† Setsuko Fujita-Becker,‡ Ciprian Neagoe,* Dietmar J. Manstein,‡ Mathias Gautel,§ and Julio M. Fernandez†

*Institute of Physiology and Pathophysiology, University of Heidelberg, Im Neuenheimer Feld 326, D-69120 Heidelberg, Germany; †Department of Physiology and Biophysics, Mayo Foundation, Rochester, Minnesota 55905; ‡Max-Planck Institute of Medical Research, D-69120 Heidelberg, Germany; and §Max-Planck Institute of Molecular Physiology, D-44202 Dortmund, Germany

Received November 20, 2001, and in revised form March 27, 2002

The PEVK domain of the giant muscle protein titin is a proline-rich sequence with unknown secondary/tertiary structure. Here we compared the force-extension behavior of cloned cardiac PEVK titin measured by single-molecule atomic force spectroscopy with the extensibility of the PEVK domain measured in intact cardiac muscle sarcomeres. The analysis revealed that cardiac PEVK titin acts as an entropic spring with the properties of a random coil exhibiting mechanical conformations of different flexibility. Since *in situ,* titin is in close proximity to the thin filaments, we also studied whether the PEVK domain of cardiac or skeletal titin may interact with actin filaments. Interaction was indeed found in the *in vitro* motility assay, in which recombinant PEVK titin constructs slowed down the sliding velocity of actin filaments over myosin. Skeletal PEVK titin affected the actin sliding to a lesser degree than cardiac PEVK titin. The cardiac PEVK effect was partially suppressed by physiological Ca^{2+} concentrations, whereas the skeletal PEVK effect was independent of $[Ca^{2+}]$. Cosedimentation assays confirmed the Ca^{2+}-modulated actin-binding propensity of cardiac PEVK titin, but did not detect interaction between actin and skeletal PEVK titin. In myofibrils, the relatively weak actin-PEVK interaction gives rise to a viscous force component opposing filament sliding. Thus, the PEVK domain contributes not only to the extensibility of the sarcomere, but also affects contractile properties.

Key Words: **connectin; actin-binding protein; entropic elasticity; atomic force microscopy; immunoelectron microscopy.**

INTRODUCTION

The scaffold of vertebrate muscle sarcomeres is built from three main filament types, actin, myosin, and titin. Titin filaments run along each half-sarcomere like a backbone (Fig. 1A), connecting the Z-disks with the myosin thick filaments (see reviews by Gregorio *et al.*, 1999; Trinick and Tskhovrebova, 1999). The extensible region of titin is located in the I-band, which also contains actin thin filaments. Near the Z-disk, titin binds to actin, which makes this titin region functionally stiff (Linke *et al.*, 1997; Trombitas and Granzier, 1997). The elastic part of titin consists of two main, structurally distinct, segments. One segment is made up of tandemly arranged immunoglobulin-like (Ig) domains, the other segment is a unique intervening sequence termed the PEVK domain (Labeit and Kolmerer, 1995). These two domain types are characteristic of the elastic filaments of both vertebrate and invertebrate muscle sarcomeres (Kulke *et al.*, 2001b). Depending on muscle type, the PEVK domain is of variable length (Labeit and Kolmerer, 1995). The shortest PEVK domain is found in vertebrate cardiac muscle (~190 amino acid residues in the so-called N2B titin isoform), whereas much longer PEVK domains reaching a length of a few thousand residues are expressed in skeletal muscle titins (N2A isoforms) (Bang *et al.*, 2001). Mammalian hearts coexpress two main titin isoforms: the N2B isoform containing the short N2B-PEVK domain and a so-called N2BA isoform containing a longer PEVK segment (Freiburg *et al.*, 2000). A peculiarity is that the shortest PEVK sequence referred to as cardiac N2B-PEVK actually is contained within all vertebrate PEVK domains. In N2A titin and N2BA titin this segment corresponds to the C-terminal ~190 residues of the PEVK region (Freiburg *et al.*, 2000).

[1] To whom correspondence should be addressed. Fax: +49 6221 544049. E-mail: wolfgang.linke@urz.uni-heidelberg.de.

1047-8477/02 $35.00

Nevertheless, we use the term cardiac (N2B)-PEVK domain throughout this study.

It is still debated whether the PEVK domain adopts a specific secondary/tertiary structure. A recent report suggested that skeletal fetal PEVK fragment has a polyproline-type II helix-like configuration (Gutierrez-Cruz *et al.*, 2001). Further, the PEVK domain contains repetitive motifs of ~26–28 residues—an arrangement that may be important for the domain's structural and functional properties (Greaser, 2001). Two types of motif have been described, one containing a relatively high number of glutamate residues (polyE segment), the other an amino acid sequence of the form P-P-A-K (PPAK motif). The short N2B-PEVK domain has five PPAK motifs but no polyE segment (Greaser, 2001). In contrast, skeletal muscle PEVK titin contains both polyE segments and PPAK motifs. Therefore, it is not unreasonable to also expect differences in PEVK function in different muscle types. In this study we report some functional differences between cardiac (constitutively expressed) and skeletal PEVK titins.

In skeletal muscle, the PEVK domain is the main determinant of titin extensibility (Linke *et al.*, 1996; Gautel and Goulding, 1996) and passive force generation (Linke *et al.*, 1996) at physiological sarcomere lengths (SLs). In cardiac muscle, the PEVK domain also provides extensibility, although cardiac sarcomeres contain an additional extensible element, a 572-residue N2B-unique sequence, which makes up for the short PEVK domain (Linke *et al.*, 1999). Both skeletal PEVK (Linke *et al.*, 1998; Trombitas *et al.*, 1998) and cardiac PEVK (Helmes *et al.*, 1999) may behave as entropic springs *in situ*. Initial evidence for this idea was provided by mechanical measurements on isolated titin molecules (Tskhovrebova *et al.*, 1997; Rief *et al.*, 1997; Kellermayer *et al.*, 1997). Recently, the elastic properties of a cloned protein construct containing cardiac N2B-PEVK domains were investigated by single-molecule atomic force spectroscopy (Li *et al.*, 2001). The results suggested that cardiac PEVK may be a random coil behaving according to entropic elasticity theory. However, the data also indicated that the domain could show mechanical conformations that—while still corresponding to a random coil—have different flexibility. It was speculated that the flexibility of cardiac PEVK titin could be enzymatically controlled, e.g., by a prolyl isomerase (Li *et al.*, 2001). A novel twist was added to this issue by the observation that cardiac N2B-PEVK, and also skeletal fetal PEVK, can interact with actin filaments (Gutierrez-Cruz *et al.*, 2001; Kulke *et al.*, 2001a; Yamasaki *et al.*, 2001). An extended analysis of the interaction between actin and skeletal PEVK sequences or cardiac (constitutively expressed) PEVK titin is presented here.

In this study we use a hybrid experimental approach to investigate PEVK titin function. First, we examine the stretch force-dependent extension of single cardiac N2B-PEVK molecules by atomic force microscopy (see reviews by Fisher *et al.*, 2000; Carrion-Vazquez *et al.*, 2000). PEVK elasticity is parameterized by calculating the bending rigidity and the contour length of the isolated domain, using polymer elasticity theory. With these parameters, we then attempt a description of the force-extension relationship of cardiac PEVK titin measured in the intact sarcomere by immunoelectron microscopy and cardiac myofibril mechanics. This approach is useful in our understanding of how mechanical properties of the single molecule may translate into the mechanical behavior of the bulk structure. In another experimental series, we consider the possibility that, in the environment of the sarcomere, PEVK titin may interact with actin filaments. To this end, recombinant cardiac and skeletal PEVK constructs are tested for their ability to slow down actin filament sliding over myosin in the *in vitro* motility assay. Actin binding to either skeletal or cardiac PEVK titin is also studied by cosedimentation assay. The combined results confirm that the molecular basis of PEVK titin elasticity may be an entropic mechanism. However, additional functions are likely to be associated with the PEVK domain and are related to the actin-binding propensity of this titin region. The interaction with actin is weaker for skeletal PEVK than for cardiac (constitutively expressed) PEVK and, only for the latter, is also Ca^{2+} dependent. These novel findings are discussed in terms of their implications for the elasticity and contractile performance of skeletal and cardiac muscles.

MATERIALS AND METHODS

Atomic Force Microscopy (AFM) of Polyproteins

Single-molecule AFM has been described elsewhere (e.g., Fisher *et al.*, 2000; Carrion-Vazquez *et al.*, 2000). The cantilevers of the force-measuring unit are standard Si_3N_4 cantilevers from Digital Instruments (Santa Barbara, CA) (spring constant, 100 mN/m) or TM Microscopes, Sunnyvale, CA (spring constant, 12 mN/m). Cantilevers were calibrated in solution using the equipartition theorem. The titin constructs used in this study are polyproteins containing either eight identical titin-Ig domains, $I27_8$ (Carrion-Vazquez *et al.*, 1999), or I27 domains interspersed with cardiac PEVK domains $(I27\text{-}PEVK)_3$ (Li *et al.*, 2001). Engineering of these polyproteins has been described in detail (Carrion-Vazquez *et al.*, 2000; Li *et al.*, 2000, 2001). We note that I27 refers to the original nomenclature of titin domains proposed by Labeit and Kolmerer (1995). Following the discovery of additional Ig domains in the human gene sequence of titin, the numbering of I27 was changed to I91 (Freiburg *et al.*, 2000; Bang *et al.*, 2001). In a typical AFM stretch experiment, 3–10 μl of protein sample

concentrated at 10–100 μg/ml was deposited onto freshly evaporated gold coverslips, and the protein was allowed to adsorb onto the gold surface. Force-extension measurements were carried out in PBS buffer at an ionic strength of 200–300 mM.

Analysis of the Stretch Force-Dependent in Situ Extension of the Cardiac PEVK Domain

Immunoelectron/immunofluorescence microscopy with titin-specific antibodies flanking the cardiac PEVK domain (I18, I20/22) was used previously to establish the extensibility of N2B-PEVK titin in rabbit cardiac muscle sarcomeres (Linke *et al.*, 1999). I18 is a monoclonal anti-mouse IgG antibody (Linke *et al.*, 1999) raised against the cardiac-specific Ig domain I18 (old nomenclature; Labeit and Kolmerer, 1995) or I26 (new nomenclature; Freiburg *et al.*, 2000). I20/22 is a polyclonal anti-rabbit IgG antibody (Linke *et al.*, 1998) raised against the constitutively expressed titin region enclosing Ig domains I20-I21-I22 (old nomenclature; Labeit and Kolmerer, 1995) or I84-I85-I86 (new nomenclature; Freiburg *et al.*, 2000). In the present study, the antibody epitope-mobility data obtained over a range of SLs, from 1.8 to 2.8 μm (Linke *et al.*, 1999), were pooled in SL bins of 50 nm. For each SL bin, the corresponding PEVK extension was measured as the distance between the mean antibody epitope positions and was plotted against SL. The stretch force needed to extend cardiac PEVK titin was determined from mechanical recordings of the passive tension of isolated rabbit cardiac myofibrils (Linke, 2000).

Actin-Myosin in Vitro Motility Assay (IVMA)

This assay was performed as described previously (Anson *et al.*, 1996; Kulke *et al.*, 2001a). Briefly, motility chambers were constructed from glass slides coated with bovine serum albumin and 18-mm-square coverslips coated with a thin nitrocellulose film. Experiments were carried out with heavy meromyosin, sometimes also whole myosin, from chicken breast muscle. Actin was prepared from rabbit back muscle. Measurements were done with pure actin filaments or tropomyosin-reconstituted F-actin. Tropomyosin was a kind gift of Dr. B. Bullard (EMBL Heidelberg, Germany). The assay was carried out on the stage of an inverted microscope (Zeiss Axiovert 135) equipped with a 40 $\times$ objective and 1.6 $\times$ lens slider. Solution composition was as in Anson *et al.* (1996). The objective was heated to 30°C by using a peltier device. Sliding of rhodamine/phalloidin-labeled actin filaments was monitored in the absence and presence of various concentrations of titin construct (10 ng/ml–100 μg/ml). Images of fluorescent actin filaments were recorded with an intensified video camera (Photonic Science) and S-VHS video recorder (JVC) via an image-processing system (Hamamatsu, Argus 20). Images could be digitized with a PC and frame-grabber board (CG7, Scion Corp.). Movies were analyzed with tracking software (http://mc11.mcri.ac.uk/Retrac) to determine the sliding speed of randomly selected actin filaments within the field of view. The number of stationary filaments was counted within a 50 $\times$ 50 μm region of interest.

Recombinant Titin Constructs in IVMA

To test whether titin domains could slow down actin sliding, various cloned constructs were added to the ATP-containing buffer infused into the motility chamber to initiate actin movement. The following construct types were used: I18/I19-I20 (old nomenclature; Labeit and Kolmerer, 1995) or I26/I27-I84 (new nomenclature; Freiburg *et al.*, 2000), which contains the cardiac PEVK domain flanked by two N-terminal Ig domains and a C-terminal Ig module; I18/I19 (I26/I27), which contains two Ig domains; and I20 (I84), which is a single Ig domain. Expression of these constructs was described previously (Kulke *et al.*, 2001a). In addition, a fragment of skeletal PEVK titin (residues 20143–23430 of human skeletal titin; EMBL Accession No. X90569; Labeit and Kolmerer, 1995) was expressed solubly in *Escherichia coli* and was prepared essentially as described (Gautel *et al.*, 1995). His_6-tagged protein was purified on Ni^{2+} NTA columns following the manufacturer's instructions (Qiagen, Germany) and further purified by anion-exchange chromatography on a monoQ column (Pharmacia, Sweden). In some experiments, the His_6 tag was cleaved off by recombinant TEV protease, without obvious effects on the binding properties. Concentration was determined by UV spectroscopy.

Actin Titin Cosedimentation Assay

This assay was performed as described (Linke *et al.*, 1997; Kulke *et al.*, 2001a). G-actin and recombinant cardiac or skeletal PEVK constructs were incubated with 50 μM $CaCl_2$ or 1 mM EGTA at 0 or 30°C. Prepared samples were separated by SDS-PAGE. PEVK titin was visualized by Western blot using 9D10 monoclonal antibody (Hybridoma Bank, University of Iowa). Scanned images were analyzed with Intelligent Quantifier software (Bioimage).

RESULTS

Single-Molecule AFM of Titin Polyproteins

The use of the atomic force microscope as a force-measuring device has allowed the study of the elastic properties of structurally distinct subsegments of titin (Fisher *et al.*, 2000). This approach overcomes interpretational limitations associated with previous single-molecule studies on whole proteins or large protein fragments (Kellermayer *et al.*, 1997; Tskhovrebova *et al.*, 1997) in that the titin domains of interest can be engineered and directly examined by AFM (Carrion-Vazquez *et al.*, 2000). For example, a single titin-Ig domain (I27 according to nomenclature by Labeit and Kolmerer, 1995; I91 according to nomenclature by Freiburg *et al.*, 2000) from the elastic region of titin (Fig. 1A) is expressed and multiplied to obtain a polyprotein containing eight serially linked I27 (I91) modules, $I27_8$ (Fig. 1C). Stretching this polyprotein in the AFM gives a characteristic "fingerprint": (1) the force-extension curve shows a sawtooth pattern, in which each peak corresponds to the unfolding of one Ig module (Figs. 1B and C); (2) the unfolding force of each peak is ~200 pN (Li *et al.*, 2000); and (3) the peaks are spaced at a constant interval (Fig. 1B). The increase in length of the polyprotein when one Ig domain unfolds can be measured with the wormlike chain (WLC) model of entropic elasticity (Bustamante *et al.*, 1994; Marko and Siggia, 1995). This model predicts that the stretch force (f) is related to the fractional extension (z/L) of the chain by

$$f = \left(\frac{k_B T}{A}\right)\left[\frac{1}{4(1 - z/L)^2} - \frac{1}{4} + \frac{z}{L}\right], \qquad (1)$$

where A is the persistence length, a measure of the chain's bending rigidity, k_B is the Boltzmann con-

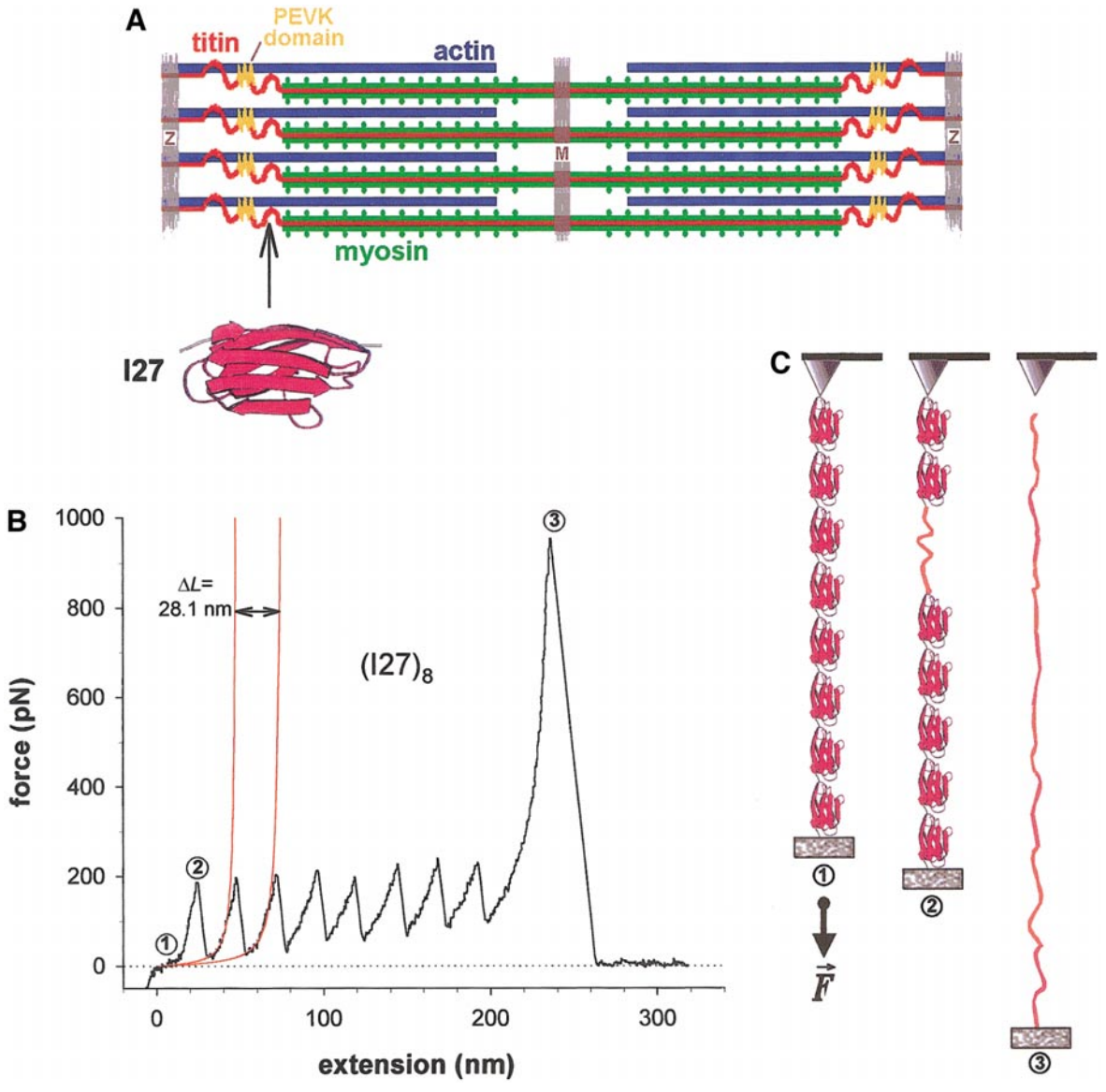

FIG. 1. Atomic force microscopy is used to investigate the force-extension behavior of cloned titin domains. (A) The immunoglobulin-like module, I27 (nomenclature according to Labeit and Kolmerer, 1995) or I91 (nomenclature according to Freiburg *et al.*, 2000), derived from the Ig region of titin located near the myosin-filament edge, can be used as a "gold standard" in single-molecule force spectroscopy measurements of titin domains. I27 (I91) structure according to Improta *et al.*, (1996). (B) Sawtooth pattern of the force-extension curve obtained when a polyprotein of the type $I27_8$ ($I91_8$) is stretched by AFM. Force peaks near 200 pN indicate Ig domain unfolding events. The last peak near 1000 pN does not correspond to an unfolding event but to rupture of the polymer from the sites of attachment. The red lines are WLC fits (Levenberg-Marquardt algorithm) based on Eq. (1), to the second and third force peak. One unfolding event is calculated to increase the contour length, L, of the polyprotein by exactly 28.1 nm. (C) Schematic of how the $I27_8$ ($I91_8$) polyprotein is attached to the AFM cantilever (top) and a gold-coated coverslip surface (bottom) and stretched by a force, F. Stages 1 to 3 correspond to the numbers above the force trace in (B).

stant, T is absolute temperature (300 K in our experiments), z is the end-to-end length (or extension), and L is the chain's contour length. Fitting this model to each sawtooth peak in the measured force trace reveals that each unfolding event increases the contour length of the polyprotein by 28.1 nm (Fig. 1B).

Since the aim of this study was the analysis of PEVK titin function, we used a recently engineered heteropolyprotein of the type $(I27\text{-}PEVK)_3$ (Li *et al.*, 2001) for AFM measurements (Fig. 2A). The cardiac PEVK domains contained within this construct are interspersed with Ig-I27 (I91) domains to distinguish, by the characteristic fingerprinting of I27,

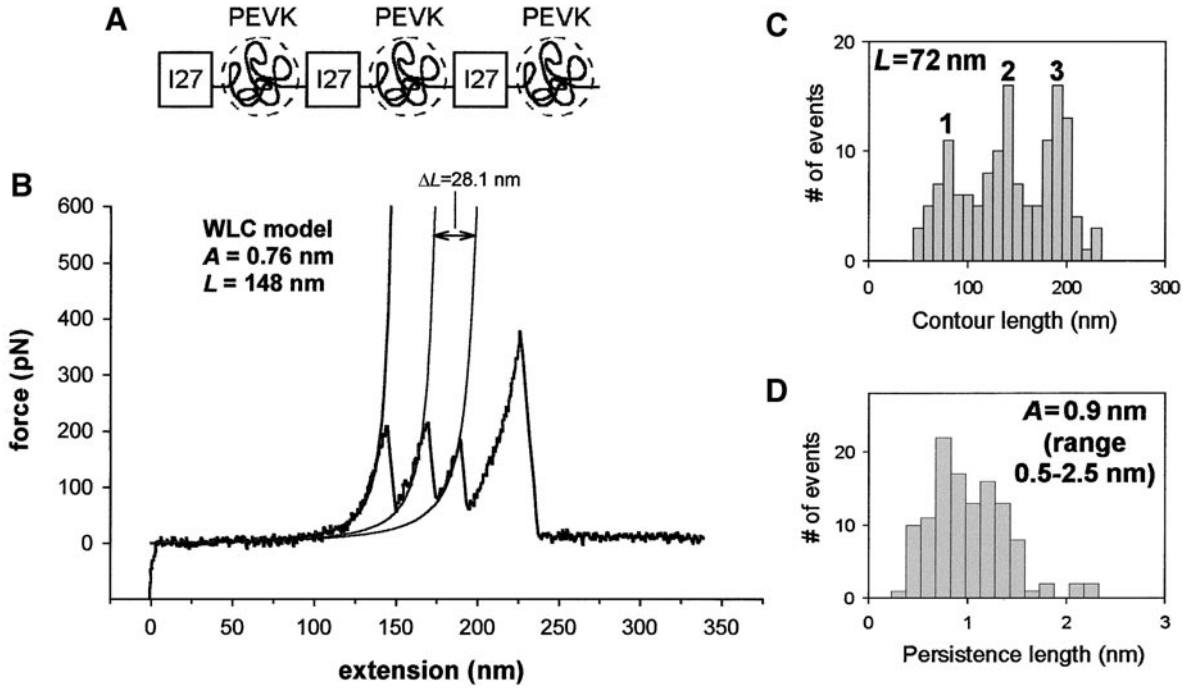

FIG. 2. AFM force spectroscopy of a heteropolyprotein containing cardiac PEVK domains. (A) Schematic of the structure of the $(I27\text{-}PEVK)_3$ polyprotein (I27 refers to nomenclature by Labeit and Kolmerer, 1995; this is I91 in the nomenclature of Freiburg *et al.*, 2000). The 186-amino acid-long N2B-PEVK domains are interspersed with I27 Ig domains (Li *et al.*, 2001). (B) Representative force-extension curve obtained by stretching a single $(I27\text{-}PEVK)_3$ molecule. A single molecule is identified by the correct spacing between force peaks (the contour-length increase, ΔL, measured by the WLC model, is 28.1 nm for one unfolding event) and the unfolding force magnitude of ~200 pN. The initial part of the force-extension curve is fitted with the WLC model (Eq. (1)) to obtain the entropic spring parameters of the PEVK domain. A persistence length, *A*, of 0.76 nm, and a contour length, *L*, of 148 nm, are calculated. In this example, the tether contained two cardiac PEVK domains and three I27-Ig modules. (C) Histogram of the contour-length distribution of single $(I27\text{-}PEVK)_3$ polyproteins examined by AFM. The average *L* of one cardiac PEVK domain is 72 nm. (D) Histogram of the persistence-length distribution of the PEVK domain extracted from measurements on single $(I27\text{-}PEVK)_3$ polyproteins.

recordings obtained from multiple polyproteins from those obtained from a single polyprotein (for details, see Li *et al.*, 2001). Only recordings obtained from single polyproteins are included in the statistical analysis (Figs. 2C and D). A typical force-extension curve of $(I27\text{-}PEVK)_3$ is shown in Fig. 2B. The force trace before the first unfolding peak corresponds to the extension of PEVK titin. In this example, the tether contained three I27 Ig modules (three unfolding peaks spaced at 28.1 nm) and two PEVK domains, as judged from the contour length, $L = 148$ nm, calculated with the WLC model; half this value would be close to the expected contour length of a fully extended PEVK domain, estimated from the number of cardiac PEVK residues (186) spaced maximally at 0.38 nm. The average contour length of one cardiac PEVK domain was 72 nm (Fig. 2C). The persistence length, A, of the PEVK domain, calculated by the WLC model, was 0.76 nm in the example of Fig. 2B and 0.9 nm on average (Fig. 2D). However, a relatively wide distribution of persistence lengths, from ~0.5 to 2.5 nm, was found (Li *et al.*, 2001). As discussed below, this wide range of persistence lengths may hint at some structural and/or functional peculiarities of the PEVK domain.

Modeling the Force-Extension Relationship of Cardiac PEVK Titin in Situ

How does the extensibility of the isolated PEVK domain measured by AFM compare to that of the PEVK domain situated in the intact cardiac muscle sarcomere? To make this comparison, we need to obtain the force-extension relationship of the N2B-cardiac PEVK domain *in situ*. In a previous work, we have used titin-specific antibodies against Ig-domains that flank the cardiac PEVK domain (I18, I20/22; Fig. 3A) to measure the stretch-dependent extension of this domain by immunoelectron/immunofluorescence microscopy on rabbit cardiac sarcomeres (Linke *et al.*, 1999). Rabbit left ventricle contains mainly the N2B titin isoform; 2% SDS-polyacrylamide gel electrophoresis (Linke *et al.*, 1997) detects only minor amounts of N2BA titin

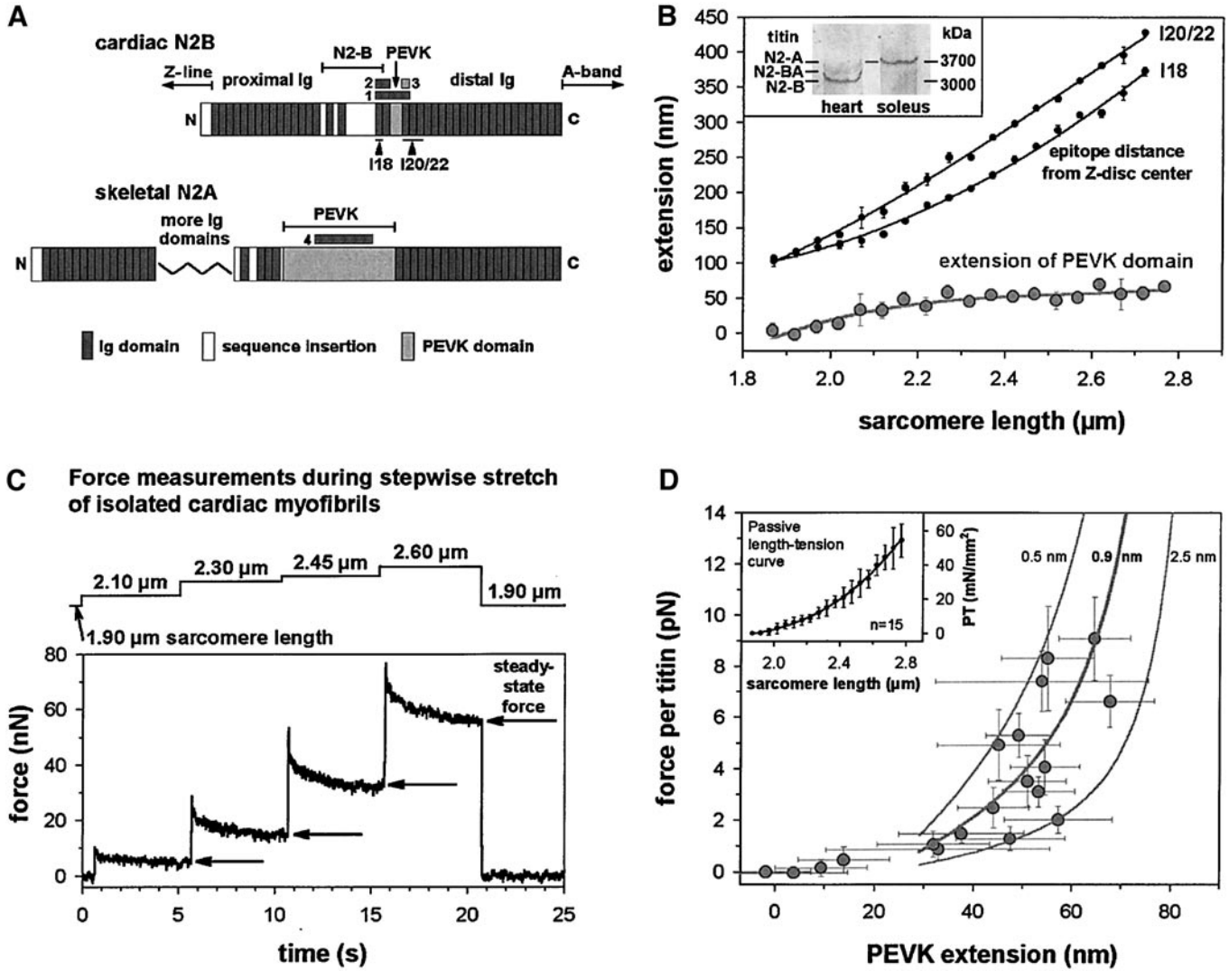

FIG. 3. Reconstitution of the extensibility of cardiac PEVK titin *in situ*, based on data sampled by AFM force spectroscopy on isolated PEVK domains. (A) Domain architecture of the extensible I-band region of titin in cardiac muscle (N2B-titin isoform) and skeletal muscle (N2A-titin isoform). The epitope positions of titin-specific antibodies (I18, I20/22) to sites near both ends of the cardiac PEVK domain are indicated by arrowheads. The thick horizontal bars numbered 1 to 4 show the sites along skeletal and cardiac titin, from which the recombinant constructs, later used in *in vitro* motility assay experiments, were derived. Nomenclature of titin domains according to Labeit and Kolmerer (1995). (B) Extension-SL curves of titin regions, established by immunoelectron/immunofluorescence microscopy on rabbit cardiac sarcomeres (Linke *et al.*, 1999). Data are means ± SEM (individual data points pooled in 50 nm SL bins); fits are third-order regressions. The SL-dependent extension of the cardiac PEVK domain was calculated from the difference between the Z-disc-to-I20 data and the Z-disc-to-I18 data, at each SL bin. Inset: Rabbit left ventricle expresses mainly the N2B-titin isoform, as detected on 2% SDS-polyacrylamide gels (*cf.* Linke *et al.*, 1997). Rabbit soleus titin band is shown for comparison. (C) Example of experimental protocol and force trace measured when nonactivated rabbit cardiac myofibrils are stretched stepwise from slack length to a series of desired SLs. The steady-state force values at the end of the hold period were used to calculate the passive length-tension curve. (D) Force-extension relationship of the PEVK domain of rabbit cardiac muscle (N2B-titin isoform) measured *in situ*. Data points are mean values and error estimates, obtained from the PEVK-extension data shown in (B) and the passive SL-tension curve shown in the inset (to calculate force per titin, we assumed a value of 6×10^9 titins per mm^2 cross-sectional area). The lines are force-extension curves calculated with the WLC model (Eq. (1)), which was fed with the parameters for persistence length (average, 0.9 nm; upper and lower extremes, 0.5 nm and 2.5 nm) and contour length (72 nm), previously established for the cardiac PEVK domain by AFM work (see Figs. 2C and D). An offset of 20 nm was added to all extension values of these WLC curves, to account for the fact that the antibody epitopes (I18, I20/22) do not directly flank the PEVK domain.

(Fig. 3B, inset). Further analysis of the immunostaining data reported previously (Linke *et al.*, 1999) reveals the mean distance of each antibody epitope from the center of the Z-disk, at successively increasing SLs (Fig. 3B, small symbols and fits). From these results, the SL-dependent extension of the cardiac PEVK domain can be calculated (Fig. 3B, large symbols and fit).

The stretch force corresponding to a given PEVK domain extension can be inferred from passive-force measurements on isolated rabbit cardiac myofibrils. The specimens are stretched stepwise and held for 5–10 s, during which stress relaxation takes place (Fig. 3C), and the near-steady-state passive force is recorded (arrows in Fig. 3C). From these data, the passive length-tension curve of rabbit cardiac myofibrils is calculated (Fig. 3D, inset; cf. Linke, 2000). The values of the measured passive tension are scaled down to the single molecule level by assuming a reasonable value of 6×10^9 titins/mm^2 cross-sectional area.

Combining the results of extensibility and force measurements on rabbit cardiac sarcomeres, we can plot the force-extension relationship of the cardiac PEVK domain *in situ* (symbols and error estimates in the main Fig. 3D). To further analyze these data points, we then apply the WLC model of entropic elasticity (Eq. (1)), using the parameters for persistence length (0.9 nm) and contour length (72 nm) previously established for cardiac PEVK titin in the AFM work. The thick line in Fig. 3D shows that the WLC fit based on these parameters connects the majority of the data points. However, some data points deviate significantly from the modeled curve, especially at higher extensions above 45 nm. Therefore, we varied the persistence-length value in the WLC model (at constant L) to test whether this could lead to a better description of the high-extension data. We used the range of persistence lengths seen in the AFM analysis (cf. Fig. 2D). The thin lines in Fig. 3D demonstrate that all data points measured *in situ* fall in between the WLC fit curves obtained with the lowest (0.5 nm) and the highest (2.5 nm) persistence-length value.

Effect of PEVK Titin Constructs on the Actin-Sliding Speed in the Actin-Myosin IVMA

In a recent study we showed that, in addition to being elastic, the cardiac N2B-PEVK domain exhibits actin-binding properties (Kulke *et al.*, 2001a). This relatively weak interaction causes a slowdown of actin sliding over myosin in the *in vitro* motility assay, because the titin construct tethers actin filaments to the surface of the motility chamber (Fig. 4A). Here, we extend this IVMA analysis and also test whether a cloned skeletal PEVK fragment can affect actin sliding. Since the recombinant cardiac PEVK titin used in the IVMA is flanked by Ig domains, we add control experiments with constructs containing either one or two Ig domains only. In Fig. 3A, the horizontal bars numbered 1, 2, 3, and 4 indicate the sites along I-band titin from which the cloned fragments used in this study were derived.

Figure 4B shows that Ig domains alone did not slow down actin filament sliding in the IVMA. In contrast, the sliding speed was affected both by cardiac PEVK and by skeletal PEVK. The effect of cardiac PEVK was stronger than that of skeletal PEVK: at a construct concentration of 1 μg/ml, car-

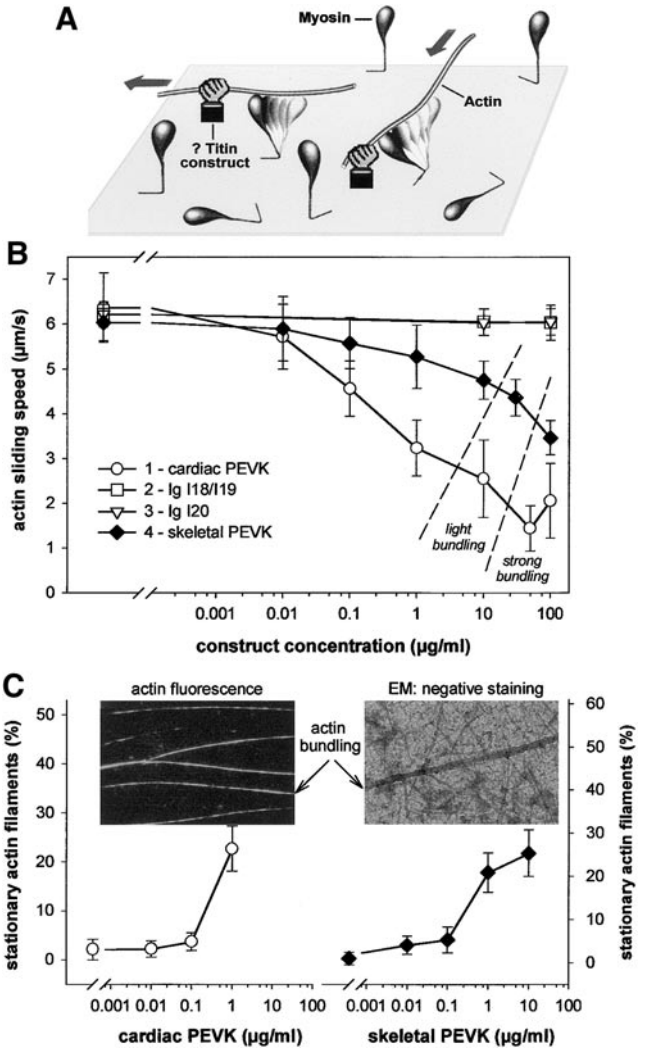

FIG. 4. Effect of PEVK titin constructs on actin-sliding speed in the *in vitro* motility assay. (A) Principle of the method. Actin-binding protein is expected to tether actin filaments to the surface of the motility chamber, thereby slowing down filament sliding. (B) Summary of the effects of four different titin constructs (cf. Fig. 3A) added to the IVMA buffer, on actin filament-sliding speed (nomenclature of titin constructs according to Labeit and Kolmerer, 1995). Only PEVK titins slow down actin sliding. The impact of cardiac PEVK domain on actin sliding is much stronger than that of skeletal PEVK fragment. (C) Effect of cardiac PEVK domain (left diagram) and skeletal PEVK fragment (right diagram) on the number of immobile actin filaments per field of view (50×50 μm). At high PEVK construct concentrations, actin bundling prevented the analysis of individual stationary actin filaments. Insets: typical images indicating actin bundling by PEVK construct. In (B) and (C), data are means $\pm$ SD, $n = 20$ actin filaments each.

diac PEVK construct inhibited the actin-sliding speed by ~50%, whereas skeletal PEVK fragment decreased the sliding speed by only ~12% (Fig. 4B). Construct concentrations above 1 μg/ml (cardiac PEVK) and 10 μg/ml (skeletal PEVK), respectively, caused various degrees of actin bundling (Fig. 4B). The observed effects of PEVK constructs on actin-sliding speed were similar when the IVMA was run with pure actin filaments or tropomyosin-reconstituted F-actin, and heavy meromyosin (HMM) or whole myosin. All data shown are from experiments with HMM and pure F-actin. The slowdown of actin sliding was accompanied by an increase in the number of immobile actin filaments (Fig. 4C). This number could be determined reliably only up to concentrations of 1 μg/ml cardiac PEVK and 10 μg/ml skeletal PEVK, as large actin bundles observable by fluorescence and electron microscopy developed at higher construct concentrations (Fig. 4C, insets). Cardiac PEVK was slightly more potent in causing actin bundling than skeletal PEVK. Altogether, the data indicated that the cardiac N2B-PEVK domain interacts more strongly with actin than skeletal PEVK domain. However, as noted in the introduction, the titin region called cardiac PEVK domain actually is part of the PEVK domain of skeletal titin isoforms also. Thus, the results may be interpreted to indicate binding of the constitutively expressed PEVK segment ("cardiac PEVK") to actin filaments in both cardiac and skeletal muscle. In contrast, PEVK sequences present only in skeletal titins may exhibit little actin-binding propensity.

Differential Effect of Ca^{2+} on the PEVK-Induced Slowdown of Actin Sliding

An intriguing observation in a recent study was that the cardiac PEVK effect on actin-sliding speed in the IVMA is partially suppressed in the presence of high [Ca^{2+}] (Kulke *et al.*, 2001a). Here we took a closer look at this phenomenon and analyzed whether Ca^{2+} interferes with the impact of both cardiac and skeletal PEVK constructs. Figure 5 demonstrates that already Ca^{2+} concentrations considered physiological (10 μM) caused a statistically significant partial reversal of the effect of cardiac PEVK (1–10 μg/ml) on actin sliding. A 100 μM Ca^{2+} further suppressed the PEVK-induced actin filament slowdown (Fig. 5). In contrast, even high Ca^{2+} concentrations of 100 μM did not alter the effect of skeletal PEVK fragment (10–30 μg/ml) on actin-sliding speed (Fig. 5). Thus, the Ca^{2+} dependency of the PEVK effect on actin sliding is specific to the N2B-PEVK domain—i.e., the constitutively expressed, ~190-residue, C-terminal region of all PEVK domains (including those of skeletal muscle titins).

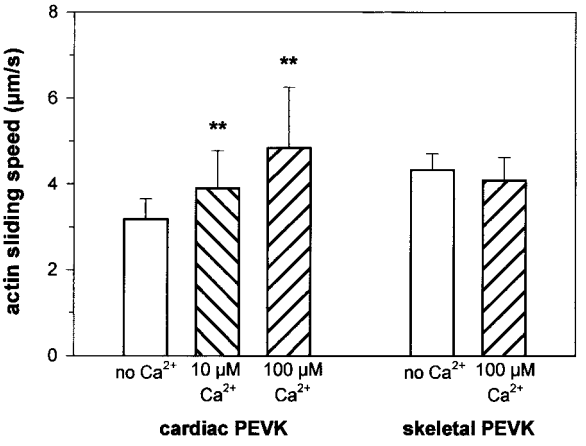

FIG. 5. Effect of Ca^{2+} on the PEVK-induced slowdown of actin filament sliding in the *in vitro* motility assay. Data are means ± SD. The impact of cardiac PEVK domain was partially reversed in the presence of Ca^{2+}, in a statistically significant manner (** $P < 0.001$ in Student's t test, versus "no Ca^{2+}" control; $n = 27–48$ analyzed actin filaments). The slowdown of actin filaments by skeletal PEVK fragment was not modified by Ca^{2+} ($n = 20$ analyzed actin filaments). Construct concentrations: cardiac PEVK, 1–10 μg/ml; skeletal PEVK, 10–30 μg/ml.

Differences in Actin-Binding Propensity between Cardiac and Skeletal PEVK Domains Are Detected by Cosedimentation Assay

In an independent test for actin-PEVK titin interaction, we employed a cosedimentation assay, in which PEVK titin was visualized by staining with anti-PEVK antibody 9D10. Figure 6A shows that this approach confirms the actin-binding propensity of the cardiac N2B-PEVK domain (including the flanking Ig domains I18/I19 (I26/I27) and I20 (I84)). The actin-PEVK association is weak at 0°C (Fig. 6A, lanes 1 and 3), but stronger at 30°C (Fig. 6A, lanes 5 and 7). The bands seen in the pellet are not just due to unspecific aggregation, as controls with no actin present revealed no signal (Fig. 6A, lane 9). Similar experiments were performed with the skeletal PEVK fragment. However, no interaction of this construct with actin was detectable, either at 0°C (Fig. 6B, lanes 1 and 3) or at 30°C (Fig. 6B, lanes 5 and 7). Sometimes, proteolytic fragments of the expressed skeletal PEVK seemed to show very weak actin interaction at 30°C (Fig. 6B, lane7), but a signal was never detected with the full-length construct (arrowhead in Fig. 6B).

In this context, we also studied whether the PEVK-actin association could be modulated by Ca^{2+}. As for the cardiac PEVK domain, the actin-binding propensity at 30°C was slightly higher in the absence than in the presence of 50 μM $CaCl_2$ (Fig. 6A, compare lanes 5 and 7). On average, a difference by a factor of 2 was found (data not

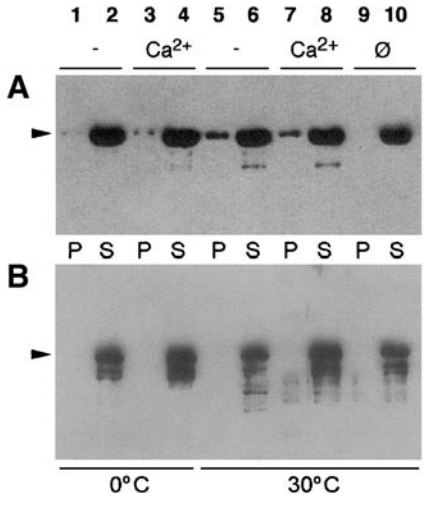

FIG. 6. Examples of Western blots documenting the results of actin-titin cosedimentation assays. (A) Association between actin and cardiac PEVK titin (including flanking Ig domains I18/I19-I20, according to nomenclature by Labeit and Kolmerer (1995) = I26/I27-I84, according to nomenclature by Freiburg *et al.*, (2000)) was probed at two different temperatures and in the presence and absence, respectively, of Ca^{2+}. Bound actin-cardiac PEVK complex was found in the pellet (position of arrowhead). (B) Similar experiments done with skeletal PEVK fragments did not detect interaction with actin (see pellet and arrowhead position). Sometimes, at 30°C, degradation products of skeletal PEVK titin appeared to bind very weakly to actin (lane 7). In A and B, monoclonal antibody 9D10 was used for visualization of PEVK titin. Buffer conditions: (−), 1 mM EGTA; (Ca^{2+}), 50 μM $CaCl_2$; at either 0°C or 30°C. P, pellet; S, supernatant; ∅, control without actin. Concentrations: titin constructs, 20 μM; actin, 40 μM.

shown). At 0°C, no obvious Ca^{2+} effect was detectable. The skeletal PEVK domain, lacking an association with actin already in the absence of Ca^{2+}, showed no change in actin-binding propensity in the presence of Ca^{2+} (Fig. 6B). In conclusion, cardiac N2B-PEVK i.e., the constitutively expressed PEVK segment), but not skeletal PEVK, interacts relatively weakly with actin in a temperature-dependent and Ca^{2+}-dependent manner.

DISCUSSION

Recent experimental work has established the PEVK domain of both cardiac and skeletal muscle titins as an extensible element that is important for the elasticity of the sarcomere (Linke *et al.*, 1996, 1998, 1999; Gautel and Goulding, 1996; Trombitas *et al.*, 1998; Helmes *et al.*, 1999; Li *et al.*, 2001). Whereas reversible extensibility of the PEVK domain has been shown unequivocally, there are open questions concerning the molecular mechanism of PEVK elasticity. From sequence analysis, it was argued that the clusters of negative charges present within the PEVK domain could act to prevent the formation of stable tertiary structural folds (Labeit and Kolmerer, 1995). In studies of the *in situ* extensibility of skeletal titin segments it was proposed that the PEVK domain could be a permanently unfolded segment exhibiting entropic elasticity (Trombitas *et al.*, 1998). Analyses of skeletal PEVK extensibility in the sarcomere, using polymer-elasticity theory, concluded that an entropic spring mechanism may indeed explain much of the elasticity of PEVK titin (Linke *et al.*, 1998). However, it was also suggested that other factors, such as electrostatic and/or hydrophobic interactions, could give rise to an "enthalpic" component of skeletal PEVK elasticity (Linke *et al.*, 1998). The possibility that PEVK elasticity may not be purely entropic was indirectly supported by a report demonstrating the propensity of a cloned skeletal fetal PEVK fragment to form a polyproline type II-like helix (Gutierrez-Cruz *et al.*, 2001). Also the discovery of 26–28 amino acid residue repeats present within the PEVK domain (Freiburg *et al.*, 2000; Greaser, 2001; Gutierrez-Cruz *et al.*, 2001) may hint at a more complex elasticity of the PEVK segment. On the other hand, bacterially expressed cardiac PEVK domain was recently studied by single-molecule AFM force spectroscopy, and was found to largely behave as a random coil (Li *et al.*, 2001). Some evidence, however, was put forth indicating that the PEVK domain may exhibit conformations of different flexibility (Li *et al.*, 2001)—a fact that perhaps translates into elastic anisotropy (cf. Linke *et al.*, 1998). In conclusion, the molecular basis of PEVK elasticity is not yet understood completely, although it seems clear that an entropic spring mechanism is at least partially involved.

The present study addresses these issues from a novel point of view. The experimental approach taken by us combines AFM mechanical measurements on single titin polyproteins with mechanical measurements on intact sarcomeres, to try to explain the molecular basis of cardiac PEVK elasticity in the environment of the sarcomere. We find that the entropic spring parameters established by AFM work for N2B-PEVK titin (persistence length, A; contour length, L) can be readily used to explain the force-extension relationship of cardiac PEVK-titin *in situ*. Interestingly, the use of a single persistence-length value (A = 0.9 nm) in the WLC model (Eq. (1)) resulted in a force-extension curve describing only part of the data points measured in intact sarcomeres (Fig. 3D). The remaining data points fell in between the force-extension curves modeled with values of A representing the longest (A = 2.5 nm) and shortest (A = 0.5 nm) persistence length, respectively, measured by AFM. These results are consistent with the idea that the cardiac PEVK domain may be an entropic spring that displays multiple

conformations of different mechanical flexibility (Li *et al.*, 2001). Thus, the present work suggests that a broad range of mechanical conformations is characteristic of cardiac (constitutively expressed) PEVK titin *in vitro* and *in situ*. It will be interesting to find out in future work whether these findings may also apply to the skeletal PEVK domain. AFM measurements on expressed skeletal PEVK titin could provide the answer to this question.

At this point it is unclear how the cardiac PEVK domain can assume various mechanical conformations. One could speculate that, at least *in situ*, the elastic behavior of this domain might be influenced in part by the weak interaction with actin (Figs. 4 and 6), which could alter the conformational freedom of the entropic spring. If actin filaments are removed from the cardiac muscle sarcomere, the force response of nonactivated myofibrils to mechanical stretch indeed changes immediately (Kulke *et al.*, 2001a). However, most or all of this rapid force decrease has been attributed to a loss of viscous drag forces originating in actin-PEVK titin interactions, and not to alterations in steady-state (elastic) force (Kulke *et al.*, 2001a). Thus, the presence of actin in the sarcomere may not significantly interfere with the (steady-state) elasticity of the cardiac PEVK domain. It seems rather unlikely that the conformations of different mechanical flexibility associated with the cardiac PEVK domain *in situ* originate in something other than the domain's intrinsic properties.

Although only recently it became clear that the cardiac (constitutively expressed) PEVK domain binds weakly to actin (this study, Figs. 4 and 6; Kulke *et al.*, 2001a; Yamasaki *et al.*, 2001), actin association with titin filaments is not a new proposal. Interaction of actin with whole titin filaments was described previously, using a variety of methods (Maruyama *et al.*, 1987; Funatsu *et al.*, 1993; Soteriou *et al.*, 1993; Kellermayer and Granzier, 1996). Actin binding was shown for a functionally stiff titin region adjacent to the Z-disc (Linke *et al.*, 1997). Some studies had also reported binding of actin to cloned Ig domains or fibronectin-type 3-like domains derived from a segment of titin near the A-band edge (Jin, 1995; Li *et al.*, 1995; Stuyvers *et al.*, 1998), but this association could not be confirmed in other studies (Linke *et al.*, 1997; Kulke *et al.*, 2001a; Yamasaki *et al.*, 2001). At this stage, it appears that interaction between the elastic titin segment and actin filaments is confined to the PEVK domain. In the present study, we explored the possibility that weak binding to actin is not only a property of the cardiac PEVK domain, but also the skeletal PEVK-rich sequences.

We found significant differences in actin-binding propensity between the two types of PEVK titin. Cardiac N2B-PEVK domain inhibited actin filament sliding over myosin in the *in vitro* motility assay more strongly than a skeletal PEVK fragment (Fig. 4). The decrease in actin-sliding speed implies an interaction between actin and either type of PEVK titin. In contrast, in cosedimentation assays, cardiac N2B-PEVK associated relatively weakly with actin, whereas skeletal PEVK did not cosediment with actin at all (Fig. 6). Possibly, the cosedimentation assay is a less sensitive method for detecting weak interaction between actin and its ligand than the IVMA technique, in which actin-binding protein effectively tethers single actin filaments to the coverslip surface (Bing *et al.*, 2000). Hence, we propose that both cardiac (constitutively expressed) and skeletal PEVK titin do associate with actin, but that the skeletal PEVK-rich sequences have a much weaker actin-binding propensity. Weak actin binding was also reported recently for an expressed skeletal fetal PEVK fragment (Gutierrez-Cruz *et al.*, 2001). We have previously discussed that the PEVK-actin association may involve both electrostatic and hydrophobic interactions, as judged from the fact that ionic conditions, as well as temperature, affect the strength of actin-cardiac PEVK binding (Kulke *et al.*, 2001a). Then, differences between skeletal and cardiac PEVK domains in terms of charge distribution and superrepeat arrangement (Yamasaki *et al.*, 2001) may be responsible for the different actin-binding propensities of these domains. However, as noted above, since the "cardiac PEVK" used here is constitutively expressed in all titin isoforms, the functions ascribed to this fragment may represent functions of all vertebrate muscle PEVK titins.

Another important difference was found between the two PEVK domains studied: the actin association of skeletal PEVK titin was independent of the Ca^{2+} concentration (Fig. 5), whereas that of cardiac N2B-PEVK was partially suppressed in the presence of 10 and 100 μM [Ca^{2+}] applied in the IVMA assay (Fig. 5) or 50 μM [Ca^{2+}] applied in cosedimentation assays (Fig. 6A). These results hint at the possibility that the actin-PEVK association is controlled in the sarcomere. Elsewhere we have shown that neither Ca^{2+}-calmodulin nor Ca^{2+}-S100 protein have additional modulatory effects on actin-cardiac PEVK binding (Kulke *et al.*, 2001a), although this finding differed from that reported by another group (Yamasaki *et al.*, 2001). These differences notwithstanding, it will be interesting to identify possible regulators of actin-PEVK interaction *in situ*. It is clear that this relatively weak interaction is important for the mechanical properties of cardiac myofibrils, as it gives rise to a viscous force component opposing filament sliding (Kulke *et al.*, 2001a).

However, viscous forces appear also in skeletal muscle sarcomeres (Minajeva *et al.*, 2001, 2002), and some of this viscosity may arise from interaction between actin and PEVK titin (Minajeva *et al.*, 2002). Since Ca^{2+} further decreases the binding strength between the actin and the PEVK domain, the viscous load could be lower during active contraction, e.g., in cardiac muscle in systole, compared to that of nonactivated muscle. Earlier mechanical work on muscle fibers indeed showed that "resting viscosity" disappears when a fiber is activated (Ford *et al.*, 1977). Follow-up studies could now test whether Ca^{2+}-regulated actin-PEVK binding may underlie this mechanical behavior.

In summary, by using a hybrid experimental approach, we studied the functional properties of the PEVK domain of titin. Single-molecule atomic force microscopy was employed to directly examine the extensibility of a polyprotein containing cardiac PEVK domains. Data obtained this way were used to explain the force-extension curve of the PEVK domain in the context of the cardiac sarcomere. We found that cardiac PEVK (a domain constitutively expressed in all titin isoforms) behaves as an entropic spring *in vitro* and *in situ*. The domain exhibits properties of a random coil that displays multiple conformations of mechanical flexibility. Cardiac PEVK was also shown to interact weakly with actin filaments in cosedimentation assays and to slow down actin-filament sliding over myosin in the *in vitro* motility assay. These effects could be partially suppressed by physiological amounts of Ca^{2+}. In contrast, a skeletal PEVK fragment had much less impact on actin-sliding speed in the IVMA; Ca^{2+} did not modify this effect. We conclude that the PEVK domain is not only a main contributor to titin elasticity, but also important as a modulator of contractile properties.

We thank Heiko Stegmann and Rasmus Schröder for providing negatively stained images of actin filaments. We acknowledge financial support of the Deutsche Forschungsgemeinschaft (Grants Li 690/5-1 and Li 690/6-2).

REFERENCES

Anson, M., Geeves, M. A., Kurzawa, S. E., and Manstein, D. J. (1996) Myosin motors with artificial lever arms. *EMBO J.* **15,** 6069–6074.

Bang, M. L., Centner, T., Fornoff, F., Geach, A. J., Gotthardt, M., McNabb, M., Witt, C. C., Labeit, D., Gregorio, C. C., Granzier, H., and Labeit, S. (2001) The complete gene sequence of titin, expression of an unusual approximately 700-kDa titin isoform, and its interaction with obscurin identify a novel Z-line to I-band linking system. *Circ. Res.* **89,** 1065–1072.

Bing, W., Knott, A., and Marston, S. B. (2000) A simple method for measuring the relative force exerted by myosin on actin filaments in the in vitro motility assay: Evidence that tropomyosin and troponin increase force in single thin filaments. *Biochem. J.* **350,** 693–699.

Bustamante, C., Marko, J. F., Siggia, E. D., and Smith, S. (1994). Entropic elasticity of λ-phage DNA. *Science* **265,** 1599–1600.

Carrion-Vazquez, M., Oberhauser, A. F., Fowler, S. B., Marszalek, P. E., Broedel, S. E., Clarke, J., and Fernandez, J. M. (1999) Mechanical and chemical unfolding of a single protein: A comparison. *Proc. Natl. Acad. Sci. USA* **96,** 3694–3699.

Carrion-Vazquez, M., Oberhauser, A. F., Fisher, T. E., Marszalek, P. E., Li, H., and Fernandez, J. M. (2000) Mechanical design of proteins studied by single-molecule force spectroscopy and protein engineering. *Prog. Biophys. Mol. Biol.* **74,** 63–91.

Fisher, T. E., Marszalek, P. E., and Fernandez, J. M. (2000) Stretching single molecules into novel conformations using the atomic force microscope. *Nature Struct. Biol.* **7,** 719–724.

Ford, L. E., Huxley, A. F., and Simmons, R. M. (1977) Tension responses to sudden length change in stimulated frog muscle fibres near slack length. *J. Physiol.* **269,** 441–515.

Freiburg, A., Trombitas, K., Hell, W., Cazorla, O., Fougerousse, F., Centner, T., Kolmerer, B., Witt, C., Beckmann, J. S., Gregorio, C. C., Granzier, H., and Labeit, S. (2000) Series of exon-skipping events in the elastic spring region of titin as the structural basis for myofibrillar elastic diversity. *Circ. Res.* **86,** 1114–1121.

Funatsu, T., Kono, E., Higuchi, H., Kimura, S., Ishiwata, S., Yoshioka, T., Maruyama, K., and Tsukita, S. (1993) Elastic filaments in situ in cardiac muscle: Deep-etch replica analysis in combination with selective removal of actin and myosin filaments. *J. Cell Biol.* **120,** 711–724.

Gautel, M., and Goulding, D. (1996). A molecular map of titin/connectin elasticity reveals two different mechanisms acting in series. *FEBS Lett.* **385,** 11–14.

Gautel, M., Castiglione Morelli, M. A., Pfuhl, M., Motta, A., and Pastore, A. (1995) A calmodulin-binding sequence in the C-terminus of human cardiac titin kinase. *Eur. J. Biochem.* **230,** 752–759.

Greaser, M. (2001) Identification of new repeating motifs in titin. *Proteins* **43,** 145–149.

Gregorio, C. C., Granzier, H., Sorimachi, H., and Labeit, S. (1999) Muscle assembly: A titanic achievement? *Curr. Opin. Cell Biol.* **11,** 18–25.

Gutierrez-Cruz, G., van Heerden, A. H., and Wang, K. (2001) Modular motif, structural folds and affinity profiles of the PEVK segment of human fetal skeletal muscle titin. *J. Biol. Chem.* **276,** 7442–7449.

Helmes, M., Trombitas, K., Centner, T., Kellermayer, M., Labeit, S., Linke, W. A., and Granzier, H. (1999) Mechanically driven contour-length adjustment in rat cardiac titin's unique N2B sequence: Titin is an adjustable spring. *Circ. Res.* **84,** 1339–1352.

Improta, S., Politou, A., and Pastore, A. (1996) Immunoglobulin-like modules from I-band titin: extensible components of muscle elasticity. *Structure* **4,** 323–337.

Jin, J.-P. (1995) Cloned rat cardiac titin class I and class II motifs. *J. Biol. Chem.* **270,** 6908–6916.

Kellermayer, M. S., and Granzier, H. L. (1996) Calcium-dependent inhibition of in vitro thin-filament motility by native titin. *FEBS Lett.* **380,** 281–286.

Kellermayer, M. S. Z., Smith, S. B., Granzier, H. L., and Bustamante, C. (1997) Folding-unfolding transitions in single titin molecules characterized with laser tweezers. *Science* **276,** 1112–1116.

Kulke, M., Fujita-Becker, S. Rostkova, E., Neagoe, C., Labeit, D.,

Manstein, D. J., Gautel, M., and Linke, W. A. (2001a) Interaction between PEVK-titin and actin filaments: Origin of a viscous force component in cardiac myofibrils. *Circ. Res.* **89,** 874–881.

Kulke, M., Neagoe, C., Kolmerer, B., Minajeva, A., Hinssen, H., Bullard, B., and Linke, W. A. (2001b) Kettin, a major source of myofibrillar stiffness in *Drosophila* indirect flight muscle. *J. Cell Biol.* **154,** 1045–1057.

Labeit, S., and Kolmerer, B. (1995) Titins, giant proteins in charge of muscle ultrastructure and elasticity. *Science* **270,** 293–296.

Li, H., Oberhauser, A. F., Fowler, S. B., Clarke, J., and Fernandez, J. M. (2000) Atomic force microscopy reveals the mechanical design of a modular protein. *Proc. Natl. Acad. Sci. USA* **97,** 6527–6531.

Li, H., Oberhauser, A. F., Redick, S. D., Carrion-Vazquez, M., Erickson, H. P., and Fernandez, J. M. (2001) Multiple conformations of PEVK proteins detected by single-molecule techniques. *Proc. Natl. Acad. Sci. USA* **98,** 10682–10686.

Li, Q., Jin, J.-P., and Granzier, H. (1995) The effect of genetically expressed cardiac titin fragments on in vitro actin motility. *Biophys. J.* **69,** 1508–1518.

Linke, W. A. (2000) Stretching molecular springs: Elasticity of titin filaments in vertebrate striated muscle. *Histol. Histopathol.* **15,** 799–811.

Linke, W. A., Ivemeyer, M., Olivieri, N., Kolmerer, B., Rüegg, J. C., and Labeit, S. (1996) Towards a molecular understanding of the elasticity of titin. *J. Mol. Biol.* **261,** 62–71.

Linke, W. A., Ivemeyer, M., Labeit, S., Hinssen, H., Rüegg, J. C., and Gautel, M. (1997) Actin-titin interaction in cardiac myofibrils: Probing a physiological role. *Biophys. J.* **73,** 905–919.

Linke, W. A., Ivemeyer, M., Mundel, P., Stockmeier, M. R., and Kolmerer, B. (1998) Nature of PEVK-titin elasticity in skeletal muscle. *Proc. Natl. Acad. Sci. USA* **95,** 8052–8057.

Linke, W. A., Rudy, D. E., Centner, T., Gautel, M., Witt, C., Labeit, S., and Gregorio, C. C. (1999) I-band titin in cardiac muscle is a three-element molecular spring and is critical for maintaining thin filament structure. *J. Cell Biol.* **146,** 631–644.

Marko, J. F., and Siggia, E. D. (1995) Stretching DNA. *Macromolecules* **28,** 8759–8770.

Maruyama, K., Hu, D. H., Suzuki, T., and Kimura, S. (1987) Binding of actin filaments to connectin. *J. Biochem. (Tokyo)* **101,** 1339–1346.

Minajeva, A., Kulke, M., Fernandez, J. M., and Linke, W. A. (2001) Unfolding of titin domains explains the viscoelastic behavior of skeletal myofibrils. *Biophys. J.* **80,** 1442–1451.

Minajeva, A., Neagoe, C., Kulke, M., and Linke, W. A. (2002) Titin-based contribution to shortening velocity of rabbit skeletal myofibrils. *J. Physiol.* **540,** 177–188.

Rief, M., Gautel, M., Oesterhelt, F., Fernandez, J. M., and Gaub, H. E. (1997) Reversible unfolding of individual titin immunoglobulin domains by AFM. *Science* **276,** 1109–1112.

Soteriou, A., Gamage, M., and Trinick, J. (1993) A survey of the interactions made by titin. *J. Cell Sci.* **104,** 119–123.

Stuyvers, B. D., Miura, M., Jin, J.-P., and ter Keurs, H. E. (1998) Ca^{2+}-dependence of diastolic properties of cardiac sarcomeres: involvement of titin. *Progr. Biophys. Mol. Biol.* **69,** 425–443.

Trinick, J., and Tskhovrebova, L. (1999) Titin: A molecular control freak. *Trends Cell Biol.* **9,** 377–380.

Trombitas, K., and Granzier, H. (1997) Actin removal from cardiac myocytes shows that near the Z-line titin attaches to actin while under tension. *Am. J. Physiol.* **273,** C662–C670.

Trombitas, K., Greaser, M., Labeit, S., Jin, J.-P., Kellermayer, M., Helmes, M., and Granzier, H. (1998) Titin extensibility in situ: Entropic elasticity of permanently folded and permanently unfolded molecular segments. *J. Cell Biol.* **140,** 853–859.

Tskhovrebova, L., Trinick, J., Sleep, J. A., and Simmons, R. M. (1997) Elasticity and unfolding of single molecules of the giant muscle protein titin. *Nature* **387,** 308–312.

Yamasaki, R., Berri, M., Wu, Y., Trombitas, K., McNabb, M., Kellermayer, M. S., Witt, C., Labeit, D., Labeit, S., Greaser, M., and Granzier, H. (2001) Titin-actin interaction in mouse myocardium: Passive tension modulation and its regulation by calcium/s100a1. *Biophys. J.* **81,** 2297–2313.